



Lithium chloride promotes osteogenesis and suppresses apoptosis during orthodontic tooth movement in osteoporotic model via regulating autophagy

Li Huang^{a,1}, Xing Yin^{a,1}, Jun Chen^b, Ruoqing Liu^a, Xiaoyue Xiao^a, Zhai Hu^a, Yan He^{c,d,*}, Shujuan Zou^{a,**}

^a State Key Laboratory of Oral Diseases, National Clinical Research Center for Oral Diseases, West China Hospital of Stomatology, Sichuan University, Chengdu, 610041, China

^b The Medical & Nursing School, Chengdu University, Chengdu, 610106, China

^c Laboratory for Regenerative Medicine, Tianyou Hospital, Wuhan University of Science and Technology, Wuhan, 430064, China

^d Department of Oral and Maxillofacial Surgery, Massachusetts General Hospital and Harvard School of Dental Medicine, Boston, MA, 02114, USA

ARTICLE INFO

Keywords:

Lithium chloride
Autophagy
Osteogenesis
Orthodontic tooth movement
Apoptosis

ABSTRACT

Osteoporosis is a widely distributed disease that may cause complications such as accelerated tooth movement, bone resorption, and tooth loss during orthodontic treatment. Promoting bone formation and reducing bone resorption are strategies for controlling these complications. For several decades, the autophagy inducer lithium chloride (LiCl) has been explored for bipolar. In this study, we investigated the autophagy-promoting effect of LiCl on bone remodeling under osteoporotic conditions during tooth movement. Ovariectomy was used to induce osteoporosis status in vivo. The results showed that LiCl rejuvenated autophagy, decreased apoptosis, and promoted bone formation, thus protecting tooth movement in osteoporotic mice. Furthermore, in vitro experiments showed that LiCl reversed the effects of ovariectomy on bone marrow-derived mesenchymal stem cells (BMSCs) extracted from ovariectomized mice, promoting osteogenesis and suppressing apoptosis by positively regulating autophagy. These findings suggest that LiCl can significantly decrease adverse effects of osteoporosis on bone remodeling, and that it has great potential significance in the field of bone formation during tooth movement in osteoporosis patients.

1. Introduction

Osteoporosis is a pathological condition wherein bone becomes weak and brittle, meaning that fracture can easily occur under normal and physiological conditions. Osteoporosis can occur in both sexes, but postmenopausal Caucasian and Asian female individuals are at the highest risk [1]. In general, bone mass reaches its peak around the age of 30 years. As aging occurs, the quantity of bone formation decreases faster than bone resorption occurs; the bone mass therefore starts to decrease, resulting in osteoporosis. Osteoporotic patients are characterized by

abnormal bone metabolism, in which a decrease in alveolar bone density is also observed [2]. Currently, there is a concomitant increase in the number of adult or elderly patients seeking orthodontic treatment to align the teeth for a better bite or to prepare the residual teeth for prosthodontic treatments and implants. Hence, the proportion of orthodontic patients with preexisting osteoporosis is growing [3]. Orthodontic tooth movement (OTM) is driven by force that initiates alveolar bone remodeling, characterized by bone formation on the tension side and bone resorption on the compression side. During orthodontic treatment, unbalanced alveolar bone remodeling is prone to occur in

Peer review under responsibility of KeAi Communications Co., Ltd.

* Corresponding author. Laboratory for Regenerative Medicine, Tianyou Hospital, Wuhan University of Science and Technology, Wuhan, 430064, China.

** Corresponding author. State Key Laboratory of Oral Diseases, West China Hospital of Stomatology, Sichuan University, No.14, 3rd Section, Ren Min South Road, Chengdu, 610041, Sichuan, China.

E-mail addresses: dentist_hwang@foxmail.com (L. Huang), yinxing@scu.edu.cn (X. Yin), lestatc@outlook.com (J. Chen), rosineliu@foxmail.com (R. Liu), xiao_19890303@foxmail.com (X. Xiao), zah121027@foxmail.com (Z. Hu), helen-1101@hotmail.com (Y. He), drzsj@scu.edu.cn (S. Zou).

¹ Li Huang and Xing Yin contributed equally to this work.

<https://doi.org/10.1016/j.bioactmat.2021.02.015>

Received 27 December 2020; Received in revised form 1 February 2021; Accepted 10 February 2021

Available online 9 March 2021

2452-199X/© 2021 The Authors. Publishing services by Elsevier B.V. on behalf of KeAi Communications Co. Ltd. This is an open access article under the CC

BY-NC-ND license (<http://creativecommons.org/licenses/by-nc-nd/4.0/>).

osteoporotic patients, resulting in accelerated tooth movement, periodontal tissue damage, and excessive alveolar bone resorption. This causes great harm to patients and leads to undesirable treatment outcomes [4,5]. Poor alveolar bone mass in osteoporotic individuals causes risks in the stability of orthodontic treatment. Therefore, providing safe and effective orthodontic treatment and preventing complications in osteoporotic patients has become an urgent problem in orthodontic treatment.

As a highly conserved intracellular catabolic process in evolution [6], autophagy can regulate cellular processes such as apoptosis, pathogen clearance, and inflammation to preserve normal physiological activities. Autophagy is also reportedly involved in the incidence and development of osteoporosis [6–8]. The autophagy level decreases significantly with aging, especially in terminally differentiated cells such as osteocytes and osteoclasts [9,10]. Decreasing the level of autophagy in bone can disturb the balance between osteoblastogenesis and osteoclastogenesis, leading to reduced osteogenic activity and resulting in a variety of bone metabolic diseases, including osteoporosis [11,12]. Hence, regulating autophagy may be a promising way to remodel osteoporotic bone. Bone marrow-derived mesenchymal stem cells (BMSCs) are multipotential cells and play a crucial role in bone homeostasis, and their role in the pathogenesis of osteoporosis has attracted considerable attention [13]. Recent studies have shown that increased BMSCs autophagy favors cellular self-renewal and differentiation and facilitates osteogenesis activity in bone [14–16]. However, the potential cellular mechanisms of osteogenesis and bone formation that are regulated by autophagy remain unclear.

Lithium chloride (LiCl) has been prescribed for the treatment of bipolar disorder for decades [17], and it reportedly has a neuroprotective function by promoting autophagy in vitro [14,18,19]. Furthermore, a previous study indicated that LiCl increased bone mass and improved fracture healing in vivo [20]. Zhu et al. considered that LiCl could stimulate the proliferation of human BMSCs [21]. LiCl regulates BMSC osteogenesis, thereby increasing the bone mass of mice via activation of the Wnt signaling cascade by inhibiting GSK-3 β [16,22]. In addition, LiCl has been reported to prevent BMSCs apoptosis induced by serum deprivation through autophagy induction [23]. As an activator of autophagy, the role of LiCl in autophagy and its relationship with apoptosis and bone remodeling during OTM in ovariectomized mice has not been clearly elucidated.

Therefore, this study aimed to determine whether LiCl could upregulate osteogenic differentiation, suppress apoptosis in BMSCs and promote bone formation, protect tooth movement in ovariectomized mice by upregulating autophagy. This was investigated under osteoporotic conditions both in vitro and in vivo.

2. Materials and methods

2.1. Animal experiments and study design

The use of C57BL/6 mice in this study was approved by the Ethics Committee of Sichuan University. All procedures were performed in accordance with the guidelines of the Animal Care Committee of Sichuan University (Ethical number: WCHSIRB-D-2018-059). A total of 42 female C57BL/6 mice (7 weeks old) were purchased from Dashuo Biology Technology (Chengdu, China) and acclimated under a 12-h light/dark cycle in a controlled environment (25–28 °C) for one week. The mice were randomly allocated into two groups: the sham operation group (n = 15) and the ovariectomy (OVX) group (n = 27).

To create osteoporotic conditions, bilateral ovariectomy was performed. Before ovariectomy, the body weights of all the mice were measured. The mice were anesthetized with 0.04 mg/g sodium pentobarbital (Propbs Biotechnology, Beijing, China) by intraperitoneal injection, and a towel was placed on the body, except the surgical area, to maintain the body temperature. To perform ovariectomy, the animal was placed in the supine position on a customized surgical table. Hair

removal and sterilization of the surgical area were performed using an animal shaver and iodophor. A 1 cm abdominal incision was made to expose and verify the ovaries on both sides, followed by ligating the oviduct and removing both ovaries. The wound was sewed layer by layer using 6-0 absorbable sutures. Animals in the sham operation group underwent all surgical procedures except for ligation of the oviduct and vessels and the excision of ovaries. The mice were then placed on an electric blanket and examined every 15 min until all mice fully recovered from anesthesia.

At 8 weeks after surgery, when osteoporosis model was established [24], the body weights of all mice were measured again. Orthodontic appliances were mounted according to our previous studies [22,25]. Briefly, a mouth-gag was customized and applied to facilitate the insertion of the OTM device. A customized nickel titanium coil spring, which generates approximately 10 g of force (measured by a vernier) to move the molar toward the incisor (Fig. 2b), was fixed with GRENGLOO (ORMCO, Orange, CA, USA) between the right maxillary first molar and incisor, except at the incisal edge. The animal conditions and appliances were monitored daily during the study. A soft diet was provided and pain management was performed on signs of discomfort 3 days after device placement. The 27 mice in the ovariectomy group were randomly divided into two subgroups: the OVX group (n = 15) and LiCl group (n = 12). The latter group was administered with LiCl (200 mg/kg/d [22,26,27], dissolved in ddH₂O) via gavage for 14 days. Mice in the OVX and sham groups received the same volume of vehicle (ddH₂O) during the experimental period. Four mice from each group were randomly selected and sacrificed at 3, 7, and 14 days after OTM.

2.2. Micro-computed tomography (micro-CT) analysis

To confirm the osteoporotic condition of mice created by bilateral ovariectomy, cervical dislocation was performed in three mice from each of the sham and OVX groups eight weeks after surgery to detect the parameters of the femoral head and alveolar bone via micro-CT scan. The trabecular bone in the central region of the femoral head (480 μ m \times 480 μ m \times 480 μ m) and interradicular area of the right maxillary first molar (350 μ m \times 350 μ m \times 350 μ m) were chosen as regions of interest (ROI) for analysis. To study the alveolar bone remodeling initiated by OTM, the mice were sacrificed 3, 7, and 14 days after orthodontic appliances were placed, and the alveolar bones were scanned. A cube of trabecular bone (150 μ m \times 150 μ m \times 150 μ m) at the apical part of the distal buccal root of the maxillary right first molar was chosen as the ROI for analysis.

All scans were performed with a micro-CT 50 system (Scanco Medical, Bruttisellen, Switzerland) in a standard resolution mode with a resolution of 2048 \times 2048 pixels and isotropic voxel size of 8 μ m. All images were used to reconstruct three-dimensional images. The following structural parameters of the ROI were calculated: alveolar bone resorption (the area from the cemento-enamel junction to the alveolar bone crest of the maxillary right first molar was defined); bone mineral density (BMD); trabecular spacing (Tb.Sp); bone volume over total volume (BV/TV); trabecular number (Tb.N) and OTM distance (distance between the nearest two landmark points a and b in the crowns of the first and second molars).

2.3. Specimen processing

After two weeks of OTM, all the animals were sacrificed. The right maxillary bones were dissected, fixed in 4% paraformaldehyde for 24 h, and decalcified in freshly prepared 10% ethylenediaminetetraacetic acid (EDTA) at room temperature for 4 weeks. Following dehydration and paraffin embedding, 4-mm serial sections along the coronal plane of the femoral metaphysis and along the sagittal plane of the upper first molar were cut with a microtome (HM 355S; Microm International, Walldorf, Germany).

2.4. Histology analysis

To observe morphological changes, samples were stained with hematoxylin and eosin (H&E) according to the manufacturer's instructions (G1120; Solarbio, Beijing, China). Alkaline phosphatase (ALP) activity was detected with NTM buffer (1 M Tris, 2 M MgCl₂, 5 M NaCl, Tween 20, and ddH₂O) and NBT/BCIP solution (Thermo Scientific, San Jose, CA, USA). A leukocyte acid phosphatase kit (386A-1 KT, Sigma-Aldrich, St. Louis, Missouri, USA) was used to detect tartrate-resistant acid phosphatase (TRAP) activity. Three sections per mouse in each group were stained with H&E, ALP, and TRAP. Each stained slide was selected at intervals of at least three sections. Slides from all individuals were stained and analyzed.

2.5. Immunohistochemistry (IHC) staining

Alveolar bones were fixed in 4% paraformaldehyde for 48 h at 4 °C. After decalcification in 15% EDTA at room temperature for 3 weeks, sections were prepared for IHC staining. Samples were incubated with Beclin-1 (dilution 1:500, ab62557, Abcam, Cambridge, UK), OPG (dilution 1:400, R1608-4, Huabio, Hangzhou, China), and RANKL (dilution 1:500, ab169966, Abcam) overnight at 4 °C. The area and the integrated optical density (IOD) of positive expression were photographed with a microscope and quantified using the Image-Pro Plus 6.0 analytic system (Media Cybernetics, Bethesda, MD, USA). The MOD was calculated as MOD = IOD/Area. The ratio of OPG/RANKL was calculated to evaluate the osteoclastic activity. Data were calculated based on three random locations from one slide and three independent experiments.

2.6. TUNEL staining

Terminal deoxynucleotidyl transferase 2-deoxyuridine 5-triphosphate nick end labeling (TUNEL) assay was performed according to the protocol (Beyotime, Shanghai, China) to detect cell apoptosis. Slides were scanned at 100 × focusing areas with the highest MVD. Then, at 200 × magnification, five fields per sample were randomly chosen to quantify TUNEL-positive cell number per 100 cells.

2.7. BMSCs culture and osteogenic differentiation

Sham and OVX mouse BMSCs were isolated and cultured as previously described [28]. Bone marrow was flushed out with Minimum Essential Medium α (MEM α, Gibco, Thermo, San Jose, CA, USA), supplemented with 100 U/mL penicillin and 100 mg/mL streptomycin (Hyclone, Utah, Logan, USA). The suspension was then plated in a culture flask and cultured at 37 °C in a 5% CO₂ incubator. The medium was changed every 3 days. When 80–90% confluence was reached, the primary BMSCs were collected with 0.25% trypsin–EDTA (Hyclone) and passaged. The second passage of BMSCs was selected for subsequent experiments [29,30]. To study the molecular mechanism of autophagy, BMSCs were treated with 5 mM LiCl (L4408, Sigma-Aldrich, St. Louis, Missouri, USA) [31,32] and 5 mM 3-Methyladenine (3-MA, M9281, Sigma-Aldrich) for 24 h [33,34] to mediate autophagy.

To induce osteogenic differentiation, BMSCs were cultured in an osteogenic medium (50 μM ascorbic acid, 10 mM β-glycerophosphate, and 10⁻⁷ M dexamethasone), which was replenished every 3 days. After a 7-day incubation period, the cells were determined by ALP activity assay (Beyotime). For ALP quantitative analysis, BMSCs were collected using an ALP assay kit (Beyotime), and the optical density (OD) was measured at 405 nm. After a 14-day incubation period, cells were stained with alizarin red S (Solarbio) according to the manufacturer's instructions. The results are presented as a percentage of the positive staining area per field of view (magnification, 100 ×).

2.8. Cell proliferation assay

The Cell Counting kit-8 (Dojindo, Kumamoto, Japan) was used to profile the effect of LiCl on BMSC proliferation. Briefly, the second passage BMSCs were seeded in 96 well plate and cultured in a 5% CO₂ incubator at 37 °C for 24 h. After that, LiCl (0, 1, 2, 5, 10 mM) supplemented with minimum essential medium (MEM) α was used to treat cells for another 24 h, followed by 3 h incubation in 10 μL CCK-8 solution supplemented with fresh MEM α at 37 °C in the dark. The absorbance was measured at 450 nm using a microplate reader (VariOskan Flash 3,001, Thermo Fisher Scientific).

2.9. Transmission electron microscopy (TEM) analysis

BMSCs from the sham, OVX, and LiCl groups were digested and washed, primary fixed in 2.5% glutaraldehyde overnight, and post-fixed in 1% osmium tetroxide for 1 h. After rinsing with phosphate-buffered saline (PBS), the samples were progressively dehydrated in a graded series of ethanol solutions (50%, 70%, 80%, 90%, 95%, and 100%), embedded in resin, and prepared for ultrathin sections. The sections were then stained with uranyl acetate and lead citrate. Finally, the ultrastructure of the BMSCs was analyzed using HT7700 TEM (Hitachi, Tokyo, Japan).

2.10. Apoptosis analysis

BMSCs were harvested and prepared according to the instructions of the Annexin V FITC Apoptosis Detection Kit (Dojindo). BMSCs were digested, washed, suspended in PBS, and counted to ensure 1 × 10⁵ cells for detection. The cell suspension was incubated with Annexin V-FITC and kept in the dark at room temperature for 15 min. Then, propidium iodide was added to the cell suspension, and apoptosis was detected by flow cytometry (BD Biosciences, Franklin Lakes, NJ, USA).

2.11. Quantitative real-time polymerase chain reaction (RT-PCR)

Total RNA was extracted with TRIzol reagent (Invitrogen, Carlsbad, CA, USA). RNA was reverse transcribed to cDNA using the Transcription First-Strand cDNA Synthesis Kit. The reaction conditions were as follows: 42 °C for 60 min, 70 °C for 5 min, and 4 °C. RT-PCR was performed in 20 μL reactions using SYBR® Premix Ex Taq™ kit (TaKaRa Bio, Otsu, Japan) and the ABI 7300 Real-Time PCR System (Applied Biosystems, USA). The housekeeping gene GAPDH was used as the control. The primer sequences are shown in Table 1. The relative mRNA expression levels were calculated using formula 2^{-ΔΔCT}.

2.12. Western blotting analysis

Protein levels were detected using western blotting. The primary antibodies used in this study were RUNX2 (dilution 1:1000; ET1612-47, Huabio), ALP (dilution 1:2,000, ET1601-21, Huabio), BMP2 (dilution

Table 1
Sequences of primers used in RT-PCR.

Gene	Forward primer sequence (5'–3')	Reverse primer sequence (5'–3')
<i>Gapdh</i>	AGTTCGGTGTGAACGGATTTC	TGTAGACCATGTAGTTGAGGTCA
<i>Runx2</i>	GCCGGGAATGATGAGAAC	TGGGGAGGATTGTGAAGA
<i>Bmp2</i>	CCACCCCAAGACACAGTT	GCACGTCCATTGAGAGAGT
<i>Opn</i>	GAGCGAGGATTCTGTGG	TCGACTGTAGGGACGATTG
<i>Atg8/LC3</i>	GTCAGATCGTCTGGCTCCG	GCTCCTATGGGGTTAGGGTC
<i>Beclin-1</i>	CTGTAGCCAGCCTCTGAAA	CCTCTTCTCTGGGTCT
<i>p62</i>	CAGCACAGGCACAGAAGA	GTCCCACCGACTCCAAG
<i>Opg</i>	GTTTCCCGAGGACCAAT	CCATTCAATGATGTCCAGGAG
<i>Rankl</i>	TGAAGACACACTACCTGACTCCTG	CCCACAATGTGTTGCAGTTC
<i>Sp7</i>	GCTGGAGAGGAAAGGG	GCCGAACAACCCAAAAT

1:1000; ER80602, Huabio), Sp7/Osterix (dilution 1:10,000; ab22522, Abcam), LC3B (dilution 1:1000; ET1701-65, Huabio), p62/SQSTM1 (dilution 1:10,000; ab91526, Abcam), Beclin-1 (dilution 1:10,000; ab62557, Abcam), and GAPDH (dilution 1:5000; ER1706-83, Huabio). Blots were incubated with horseradish peroxidase-conjugated goat anti-rabbit IgG secondary antibody (dilution 1:10,000, L3012, SAB, College Park, MA, USA). After normalization to GAPDH, the intensity of each band was quantified using ImageJ (National Institutes of Health, Bethesda, MA, USA).

2.13. Statistical analysis

All data in this study are reported as the mean ± standard deviation (SD) for at least three independent experiments. Student’s *t*-test or analysis of variance (ANOVA) was used for comparisons between two groups or among multiple groups. Two-way ANOVA was used for comparisons between groups at different time points. Analyses were performed using the statistical package SPSS 11.5 (SPSS, Chicago, IL, USA). Differences were considered significant at *P* < 0.05.

3. Results

3.1. Ovariectomy induced osteoporosis in mice

To assess the osteoporosis caused by bilateral ovariectomy, we compared the body weight gain and trabecular bone density of both the femur head and alveolar bone between the OVX and sham groups. Eight weeks post-operation, the weight gain of OVX mice was significantly higher than that of the sham group (Fig. 1b). Osteoclasts are clearly visible in the cancellous bone of both groups (Fig. 1c, indicated with black arrows). Micro-CT revealed a sparser trabecular bone in the femoral head of the OVX group (Fig. 1d). Meanwhile, the BMD and BV/TV of the OVX group were decreased, Tb. Sp value was increased (Fig. 1e). When observing the microarchitectural changes in alveolar bone, we found that the trabecular parameters (BMD, BV/TV, and Tb.N) of OVX mice were significantly decreased compared with those of the sham group (Fig. 1f and g). All results indicated obvious bone mass loss and trabeculae deterioration in the femoral head and alveolar bone of mice that underwent bilateral ovariectomy (Supplementary Tables 1–3).

3.2. Ovariectomy negatively affected the OTM in mice

As shown in the CT reconstruction images (Fig. 2d), alveolar bone resorption was observed. Alveolar bone resorption area in the OVX

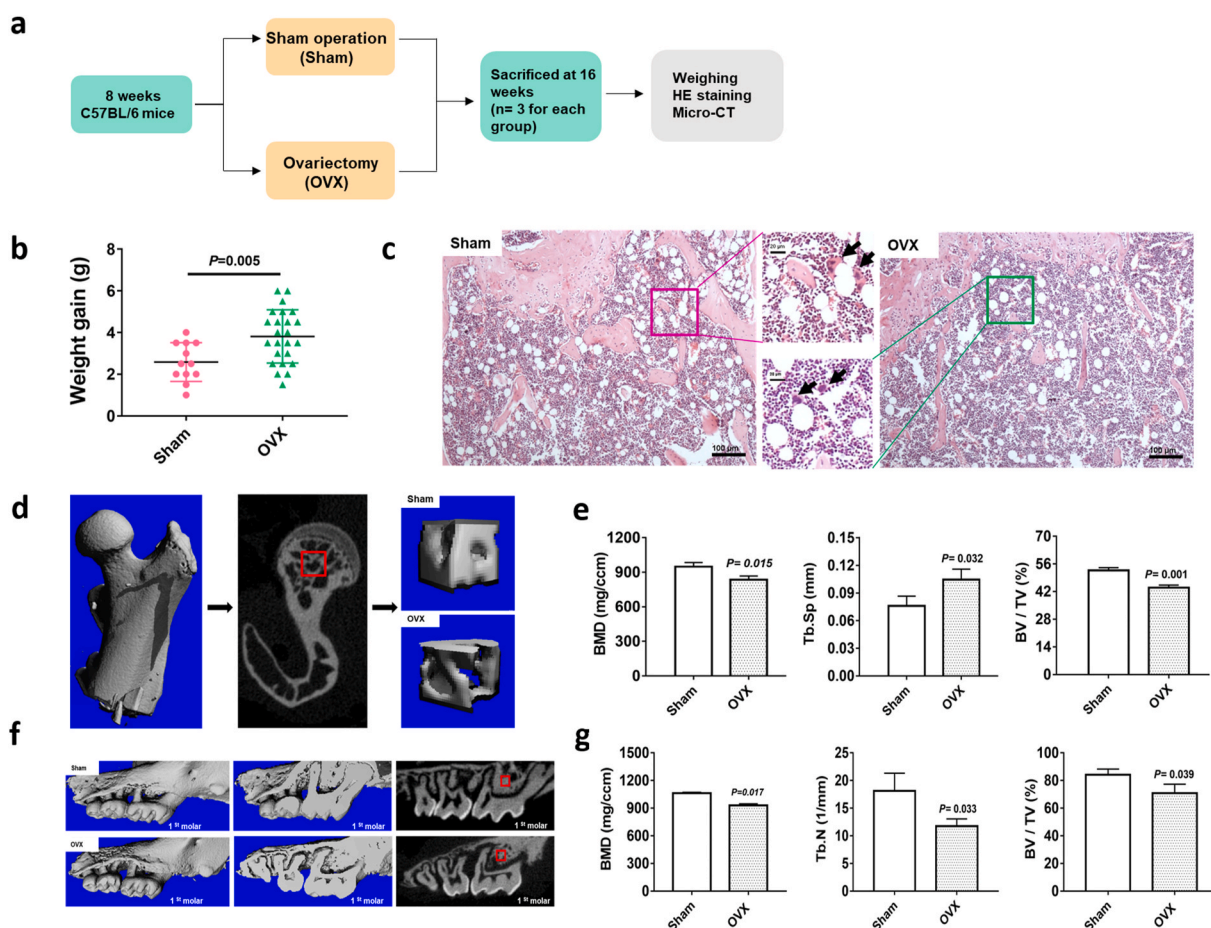


Fig. 1. Effect of ovariectomy on body weight gain and bone trabecular parameters in mice. **a**, a flowchart of the in vivo study. **b**, The weight gain in the sham and OVX groups. **c**, H&E staining of metaphysis showed in the sham and OVX mice. The black arrows indicated osteoclasts. **d**, The regions of interest (ROI) in the femur head of the sham and OVX groups. **e**, The bone volume/total volume (BV/TV) ratio, trabecular separation (Tb.Sp) and trabecular number (Tb.N) of the femur head of ROIs in the OVX and sham groups. **f**, Images of 2D and 3D of alveolar bone by rebuilding of micro-CT in the sham and OVX mice. The red boxes indicated ROI in alveolar bone. **g**, The bone mineral density (BMD), bone volume/total volume (BV/TV) ratio and trabecular number (Tb.N) in the ROI of alveolar bone in OVX and sham groups. Data represent means ± S. D (n = 3). (For interpretation of the references to colour in this figure legend, the reader is referred to the Web version of this article.)

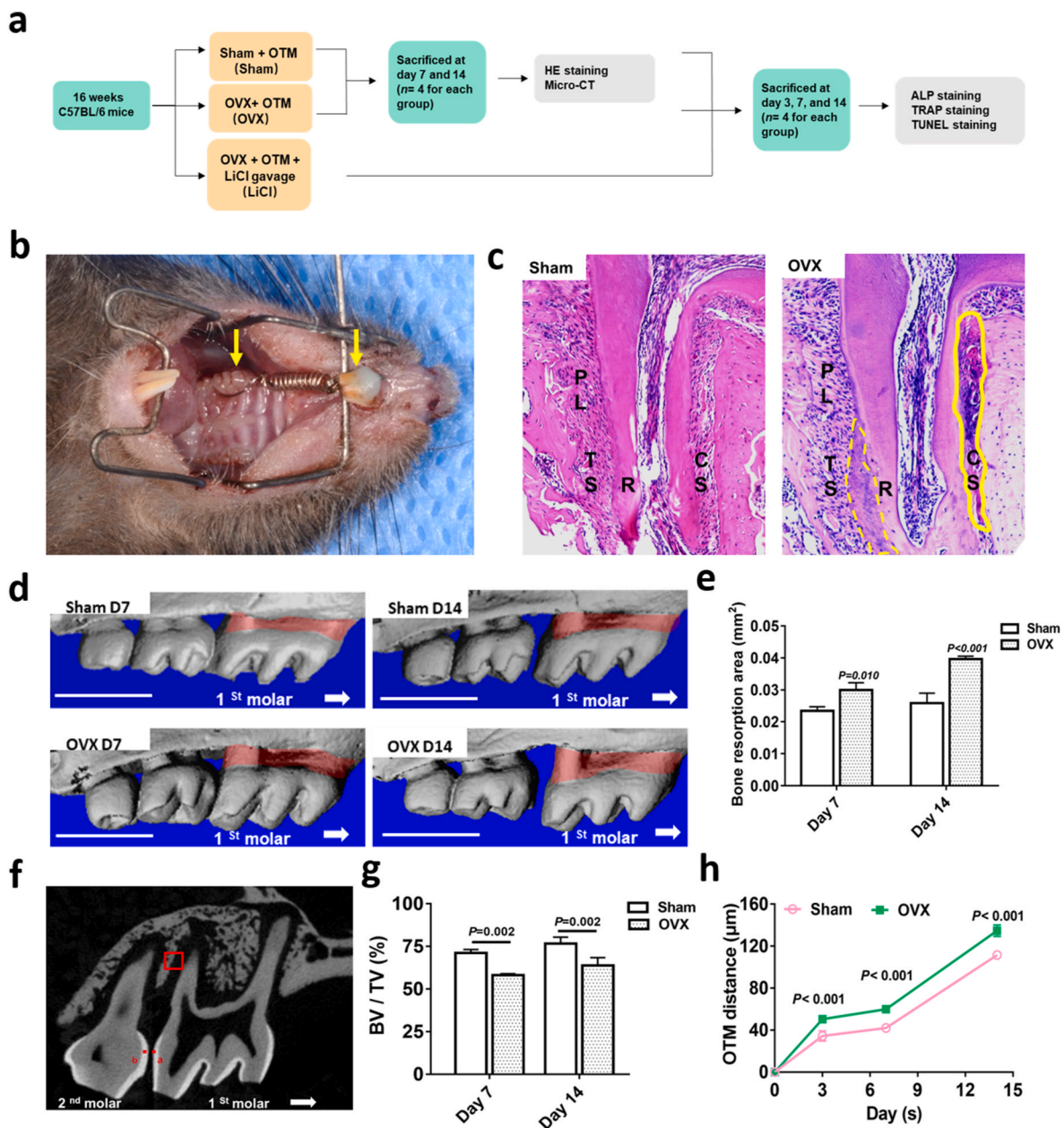


Fig. 2. Ovariectomy increased OTM distance and bone resorption in mice. **a**, a flowchart of the in vivo study. **b**, Orthodontic tooth movement (OTM) model. The left yellow arrow indicated the right upper first molar. The right yellow arrow indicated the upper incisor. **c**, Representative images of H&E staining of tooth movement on day 14 in the sham and OVX mice. The solid yellow box at the pressure side indicated hyaline change. The dotted yellow box at the tension side indicated hypercementosis. TS, the tension side; CS, the compressive side; PL, periodontal ligament; R, root. **d**, Three-dimensional reconstruction of the maxilla samples from the sham and OVX groups. Vertical bone resorption was indicated by the red-marked area. Scale bar: 1 mm. **e**, Quantification of vertical bone resorption in different groups. **f**, Sagittal view of landmark point locations and method for the measurement of OTM distance in micro-computed tomography images. Landmark points a and b were indicated. The red box indicated ROI in alveolar bone. **g**, The value of BV/TV around the apical part of the distal buccal root of the maxillary right first molar. **h**, The OTM distance in the sham and OVX groups. Data represent means \pm S. D. ($n = 3$). (For interpretation of the references to colour in this figure legend, the reader is referred to the Web version of this article.)

group was significantly larger than that in the sham group on both days 7 and 14 (Fig. 2e). Meanwhile, the BV/TV at the ROI was statistically lower in the OVX group than in the sham group (Fig. 2g), indicating that the OVX group experienced more bone resorption during OTM. Moreover, the upper first molars of the OVX group moved greater distances than those in the sham group (Fig. 2h, Supplementary Table 4), indicating that the tooth moved faster. In addition, H&E slides on day 14 showed obvious hyaline changes (Fig. 2c, indicated with a solid yellow box) on the pressure side of the periodontal ligament and hypercementosis (Fig. 2c, indicated with dotted yellow box) around the apex

area in the OVX group. The results indicated that preexisting osteoporosis conditions produced adverse effects on OTM in mice.

3.3. LiCl promoted bone formation and alleviated bone resorption in osteoporotic alveolar bone during OTM

To evaluate how LiCl affects osteoporotic alveolar bone remodeling during OTM, we performed ALP staining (Fig. 3a), which is a hallmark of osteogenesis, and TRAP staining (Fig. 3c), which represents osteoclastic activities. On day 14, ALP expression in the OVX group was the lowest,

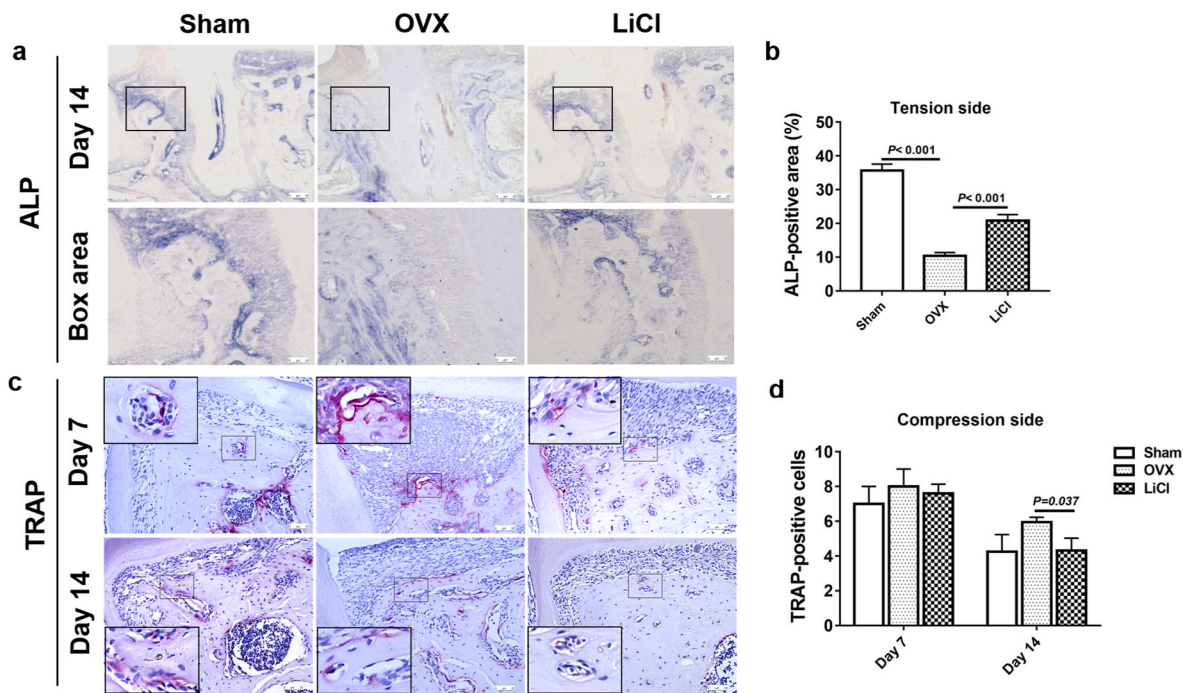


Fig. 3. LiCl promoted bone formation and inhibited bone resorption during OTM in alveolar bone. **a**, Representative images of ALP staining in the tension area on day 14 of OTM in different groups.Box area showed high-magnification images in different groups respectively. **b**, Quantitative analysis of the ALP activity. **c**, TRAP-positive cells in the pressure area on day 7 and 14 in different groups. **d**, Quantitative analysis of the TRAP positive cell number. Data represent means \pm S. D (n = 3). (For interpretation of the references to colour in this figure legend, the reader is referred to the Web version of this article.)

indicating very poor bone formation activity (Fig. 3b). The ALP-positive area in the LiCl group was significantly higher than that in the OVX group (Fig. 3b), suggesting that 14-day consecutive administration of LiCl could effectively restore bone formation in preexisting osteoporotic alveolar bone.

On the compression side, multinucleated cells, osteoclasts, appeared around the resorption lacunae in the alveolar bone (Fig. 3c). On day 7, when fast OTM occurred in all groups, the number of TRAP-positive cells in the sham, OVX, and LiCl groups was similar. As OTM slowed down on day 14, the number of TRAP-positive cells in the sham and LiCl groups

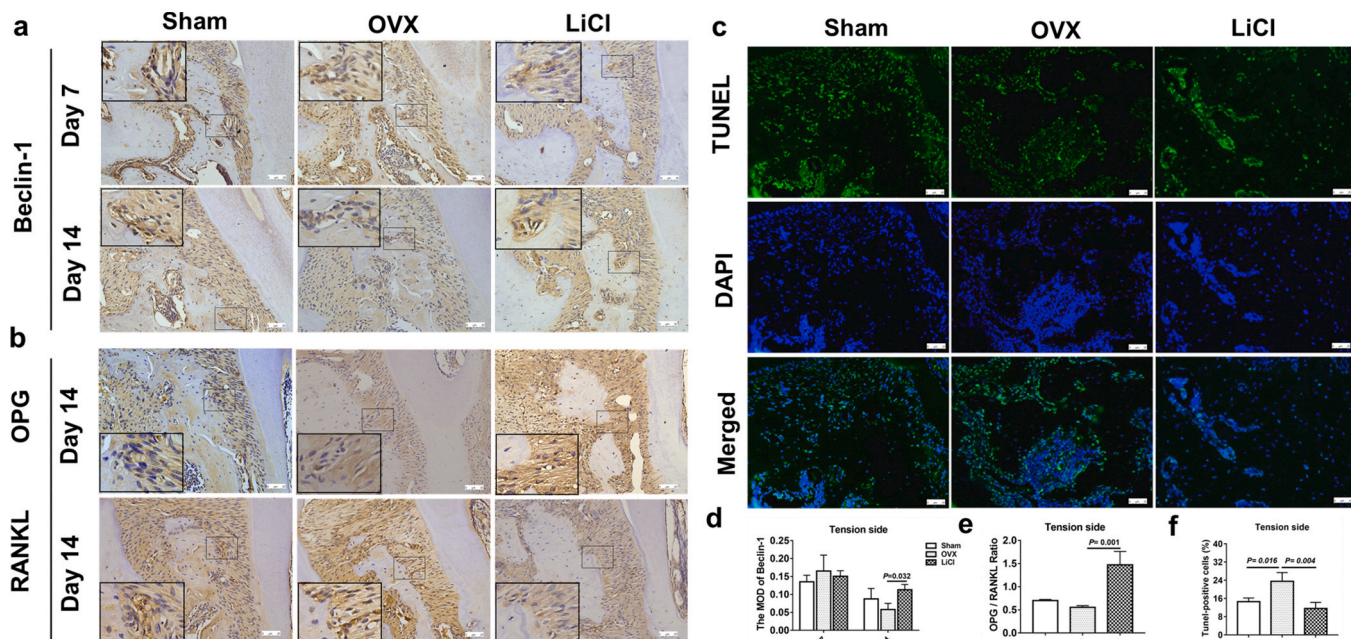


Fig. 4. LiCl promoted autophagy, inhibited apoptosis and osteoclastogenesis during OTM in mice. **a**, Immunohistochemical staining of Beclin-1 in the tension area of OTM in different groups on day 7 and day 14. **b**, Immunohistochemical staining of OPG and RANKL in the tension area during OTM in different groups on day 14. **c**, TUNEL examination of cell apoptosis in the tension side area on day 3. Green fluorescence represents apoptotic cells. **d**, The MOD of Beclin-1 in the tension area on day 7 and day 14. **e**, The ratio of OPG/RANKL in the tension area during OTM on day 14. **f**, Quantification analysis of the apoptotic cells. Data represent means \pm S. D (n = 3). (For interpretation of the references to colour in this figure legend, the reader is referred to the Web version of this article.)

was reduced by half compared to that on day 7. In contrast, the number of TRAP-positive cells in the OVX group was the highest among the three groups (Fig. 3d). These results implied that LiCl treatment could help limit bone resorption under osteoporotic conditions to a level similar to that observed in healthy individuals.

3.4. LiCl promoted autophagy and inhibited apoptosis and osteoclastogenesis in alveolar bone during OTM

As demonstrated in previous studies, we confirmed that osteoporosis (OVX group) could negatively affect the alveolar bone remodeling of OTM, resulting in ongoing bone resorption at high levels and bone formation at a very low level (Figs. 2 and 3). LiCl could minimize the influence of preexisting osteoporosis and boost alveolar bone remodeling to an almost normal level in the sham group. To further determine whether and how autophagy plays a role in the interaction between LiCl and alveolar bone remodeling during OTM in osteoporotic mice, IHC staining was used to detect the expression of Beclin-1 (Fig. 4a), which is an important autophagy-related biomarker [35] involved in the initial and late stages of autophagosome formation. On day 7, a high level of positive Beclin-1 expression was observed at the tension side in all three groups, when most cellular activity occurred in response to orthodontic force. From days 7 to 14, Beclin-1 expression decreased in all three groups, decreasing the most in the OVX group ($P = 0.074, 0.018, 0.040$ in the sham, OVX, and LiCl groups, respectively). In contrast, LiCl maintained Beclin-1 expression on day 14 at a level similar to that in the sham group ($P = 0.468$). This echoed the ALP activity on the tension side on day 14, when the ALP-positive area in the LiCl group was significantly higher than that in the OVX group (Fig. 4b). This high level of Beclin-1 expression in the LiCl group meant that LiCl could upregulate autophagy in osteoporotic mice and promote bone formation.

The expression of OPG and RANKL on the tension side 14 days after OTM was also examined by IHC staining and semi-quantitatively analyzed (Fig. 4b). The OPG/RANKL ratio was used to assess osteoclast differentiation and function [36]. We found that LiCl significantly

increased the OPG/RANKL ratio in osteoporotic mice (Fig. 4e), implying that osteoclast activity was inhibited [37].

Moreover, the effect of LiCl on the apoptotic status of the alveolar bone on the tension side was also investigated. We performed fluorescent TUNEL staining and quantified the number of TUNEL-positive cells (Fig. 4c). TUNEL-positive cells in the OVX group were at the highest level three days after OTM (Fig. 4f), and the number of positive cells between the sham and LiCl groups was similar. This finding corresponded with the observed results for Beclin-1 expression.

3.5. LiCl promoted proliferation and osteogenesis by enhancing autophagy and inhibiting apoptosis in BMSCs

The CCK-8 assay was used to detect the effect of different concentrations of LiCl on BMSCs proliferation. When the concentration was less than 5 mM, cell viability was enhanced along with the CCK-8 concentration. When the concentration reached 10 mM, BMSCs viability was significantly inhibited (Fig. 5a). Hence, 5 mM LiCl was chosen for subsequent experiments. The results revealed that 24 h of stimulation with 5 mM LiCl decreased the apoptosis level of BMSCs from ovariectomy-induced osteoporotic mice (Fig. 5b and c).

To evaluate the mineralization capacity of BMSCs, ALP staining and alizarin red S staining were performed (Fig. 5d). The bone formation capacity of BMSCs from osteoporosis mice in the OVX group was visibly hampered. However, this condition was significantly reversed when LiCl was applied to the LiCl group (Fig. 5e). TEM was used to confirm the influence of LiCl on the formation of autophagosomes and autolysosomes. The images showed that autophagosomes with double-limiting membrane in the cytoplasm of BMSCs were observed upon LiCl administration, indicating that autophagy was enhanced (Fig. 5f).

To further confirm whether autophagy of BMSCs was activated by LiCl, the autophagy-related biomarkers, the gene and protein levels of Beclin-1, LC3, and p62 were examined; these factors are critical in autophagic activity. Compared with the gene and protein expression of Atg8/LC3 and Beclin-1 of BMSCs in the OVX group, LiCl rejuvenated the

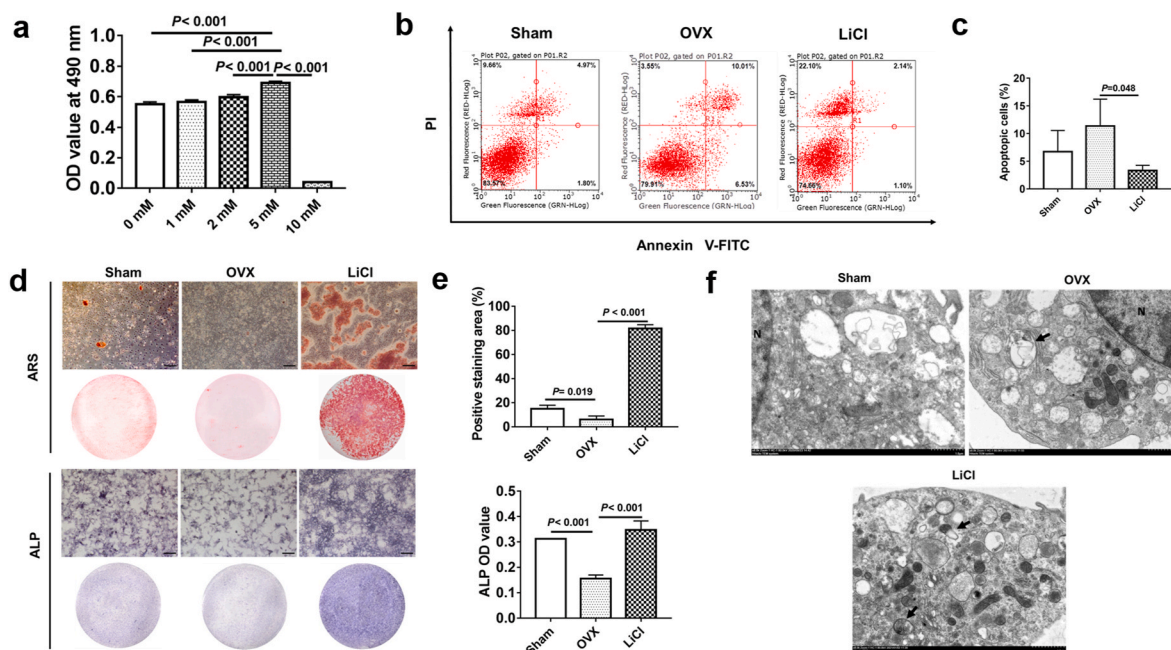


Fig. 5. LiCl promoted osteogenesis and autophagy while inhibited apoptosis in BMSCs. **a**, The OD value at 490 nm with different concentration of LiCl. **b**, Dot plot of FITC-Annexin V (x axis)/PI (y axis) of BMSCs in different groups. **c**, Quantitative analysis of apoptotic cells in different groups. **d**, After 14-day and 7-day osteogenic induction respectively, representative images of ARS and ALP activity of BMSCs in different groups. **e**, Quantitative analysis of the mineralization and the ALP activity showed that BMSCs in LiCl treated group had a significant high bone formation performance than the OVX group did. **f**, The representative morphology of autophagic vacuoles as autophagosomes was observed by TEM. Arrows indicate an autophagosomes with double-limiting membrane. N: nucleus. Scale bar, 1 μ m. Data represent means \pm S. D (n = 3).

expression of these biomarkers in the LiCl group. Meanwhile, the gene and protein levels of p62 were decreased in the LiCl group (Fig. 6a, c, and 6d). These results confirmed that LiCl promoted autophagy.

To study how LiCl affected the osteogenic ability of BMSCs from osteoporotic individuals, the osteogenesis-related genes and proteins were analyzed. Compared with those in the OVX group, the mRNA expression of *Runx2*, *Alp*, *Opn*, *Bmp2*, and *Opg* of BMSCs from the LiCl group were significantly elevated (Fig. 6b), but the ratio of *Opg*/*Rankl* increased (Supplementary Table 5). Meanwhile, the protein expression levels of ALP, OSX, and RUNX2 in BMSCs from the LiCl group were effectively enhanced by 24 h of LiCl treatment (Fig. 6e).

3.6. 3-MA blocked the pro-osteogenic effect of LiCl by downregulating autophagy in BMSCs

To further understand the mechanism underlying autophagy in BMSCs, we used the autophagy inhibitor 3-MA to mediate autophagy in BMSCs for 24 h. We found decreased mRNA expression of *Beclin-1* and *Atg8/LC3* and increased *p62* mRNA levels (Fig. 7a), in addition to decreased *Runx2*, *Bmp2*, and *Sp7* mRNA levels (Fig. 7b). Consistent with the RT-PCR results, the protein level of p62 was increased (Fig. 7d), while *Beclin-1* and LC3II protein levels were both decreased (Fig. 7d). OSX, ALP, and BMP2 levels followed a similar pattern upon 3-MA treatment (Fig. 7e).

4. Discussion

Osteoporosis is a systemic bone disorder marked by a progressive decrease in the bone trabecular number and low bone mass [2,38], and it has become a widespread problem. Osteoporosis significantly reduces the quality of life and longevity of patients [6]. As a process involving bone remodeling, OTM is also affected by this disease [39]. It has been reported that the number of osteoclasts in the periodontal tissue increased in OVX rats, which was accompanied by accelerated OTM [40]. Meanwhile, increased resorption of the alveolar bone and continued deterioration of the bone microstructure was observed [41]. OVX mice showed decreased BV/TV ratio, Tb.N, and BMD values, but an increased Tb. Sp value and OTM distance compared to those of the sham group. These results are in accordance with previous data [42]. In addition, more alveolar bone resorption can be clearly observed around

the first molar, which increases the risk of tooth loss. Hence, an increased understanding of the molecular mechanisms related to bone remodeling during OTM in osteoporosis is critical for developing efficient biological therapies to solve the problems involved.

At present, parathyroid hormone (PTH) [43], bisphosphonates [44] and alendronate [39] are common drugs for treating osteoporosis in the clinic. It has been demonstrated that these medicines have bidirectional regulatory effects that simultaneously inhibit osteoclastic activity and promote osteogenesis. Previous studies have shown that LiCl not only has a robust anabolic effect similar to PTH in bone formation in mice [20], but also promotes implant osseointegration as effectively as bisphosphonates in OVX rats [42]. Moreover, LiCl can suppress osteoclastogenesis and osteoclastic bone resorption [45,46]. Local inflammatory reactions during OTM increase the risk of periodontal tissue destruction and alveolar bone absorption in osteoporotic patients [4]. To perform a safe and smooth OTM, it is important to control osteoclastic activity in patients with osteoporotic conditions. In this study, we found fewer TRAP-positive cells on the compression side of the alveolar bone during OTM (Fig. 2c and d), which indicated that LiCl could effectively inhibit osteoclastic activity and bone resorption. In this regard, we believe that LiCl might be a promising therapeutic agent to attenuate OTM-induced bone resorption and accelerated tooth movement in osteoporotic patients receiving orthodontic treatment.

LiCl is an activator of the Wnt signaling cascade, which inhibits glycogen synthase kinase-3beta (GSK-3β) and facilitates bone formation [47]. In an in vivo study, LiCl was shown to increase bone regeneration in osteoporotic rats [48]. LiCl reduced orthodontically induced root resorption (OIRR) [49] and it has also reportedly promotes cementoblast proliferation and periodontal ligament stem cell differentiation [50,51]. In this study, we found that LiCl treatment in osteoporotic mice increased ALP staining in the tension area during OTM, which demonstrated that alveolar bone formation was promoted. LiCl has been used to regulate autophagy in neuropsychiatric diseases [52]. In vitro studies have shown that LiCl can induce autophagy, decrease apoptosis, and reduce cell damage [23,53]. Autophagy is considered important for preserving bone homeostasis [54] and plays a key role in osteoporosis [6]. However, its role in autophagy related to bone remodeling has not been extensively studied. In this study, we mainly focused on the regulation of autophagy by LiCl during bone remodeling. LC3, *Beclin-1*, and p62/SQSTM1 (p62) are autophagy biomarkers that are highly

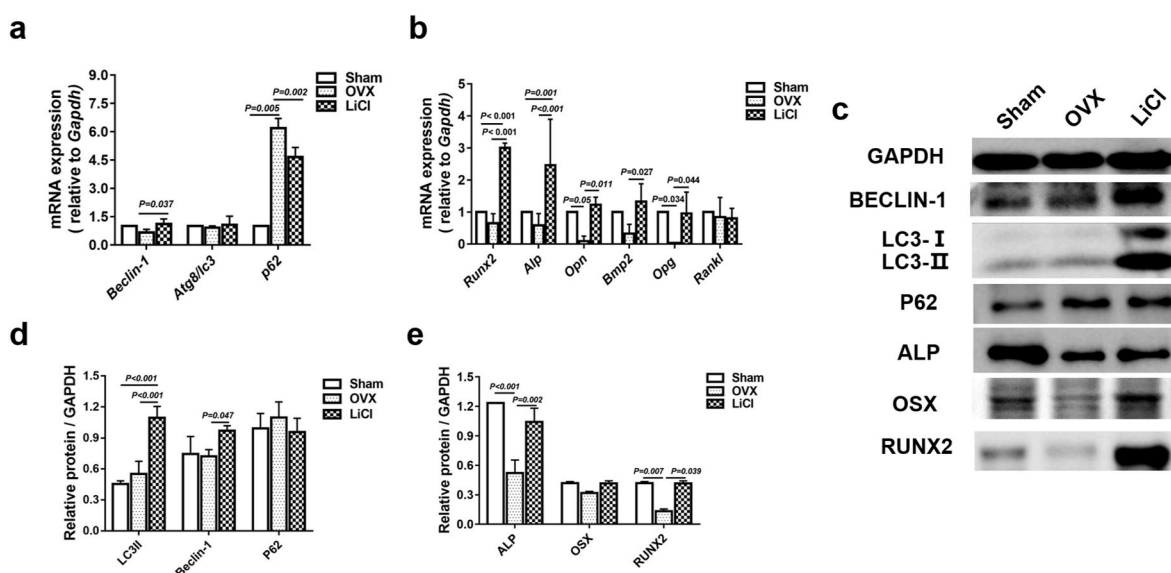


Fig. 6. LiCl promoted osteogenesis in OVX BMSCs by regulating autophagy. **a**, Real-time qPCR analyses of *Beclin-1*, *Atg8/LC3*, and *p62* mRNA expression in different groups. **b**, Real-time qPCR analyses of *Runx2*, *Alp*, *Opn*, *Opg*, and *Rankl* expression in different groups. **c**, Western blotting analysis of BECLIN-1, LC3II, p62, ALP, OSX and RUNX2 in different groups. **d**, Quantification analysis of the expression of BECLIN-1, LC3II and p62 protein. **e**, Quantification analysis of the expression of ALP, OSX and RUNX2 protein. Data represent means \pm S. D ($n = 3$).

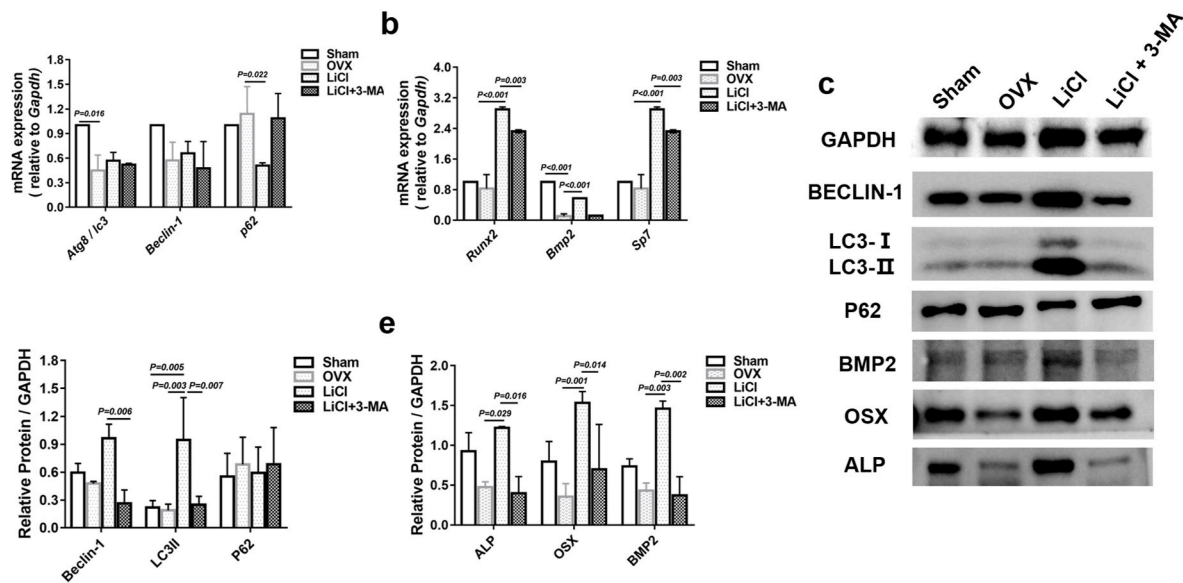


Fig. 7. The Effect of LiCl on autophagy and osteogenesis in OVX BMSCs was blocked by 3-MA. **a**, Real-time qPCR analyses of *Atg8/LC3*, *Beclin-1*, and *p62* mRNA expression in different groups. **b**, Real-time qPCR analyses of *Runx2*, *Bmp2* and *Sp7* expression in different groups. **c**, Western blotting analysis of BECLIN-1, LC3II, p62, BMP2, OSX and ALP in different groups. **d**, Quantification analysis of the expression of Beclin-1, LC3II, and P62 protein. **e**, Quantification analysis of the expression of ALP, OSX, and BMP2 protein. Data represent means \pm S. D (n = 3).

involved in autophagy. Beclin-1 is a key regulator and an indispensable component of autophagy [55]. LC3 is specifically related to autophagosome formation and is used as a marker of autophagosome accumulation [56]. P62 is regarded as an index of autophagic degradation and negatively correlates with autophagy [57]. In this study, we demonstrated that LiCl positively regulated the decrease in autophagy induced by osteoporosis. Furthermore, with LiCl application, increased levels of these biomarkers were blocked by the autophagy inhibitor 3-MA, which indicated that LiCl played a role in bone remodeling by regulating autophagy level. With the promotion of autophagy by LiCl administration, osteogenesis-related biomarkers were significantly promoted. Interestingly, the expression of osteogenic markers of BMSCs after LiCl stimulation did not proportionally increase with the level of autophagy. Compared with the OVX group, mRNA expression of the autophagy-related biomarkers *Atg8/LC3* and *Beclin-1* was increased at a low level in the LiCl group; however, the mRNA expression of osteogenesis-related biomarkers *Runx2*, *Alp*, *Opn*, and *Bmp2* increased at a high level. This may be explained by the fact that LiCl promotes osteogenic differentiation via the Wnt signaling cascade [47], suggesting that LiCl does not increase osteogenesis via a single pathway; instead, autophagy is just one of the ways in which LiCl mediated osteogenic ability [58]. Further investigation is needed to fully elucidate the activity of LiCl actions. Li et al. reported that LiCl attenuated BMP-2 signaling and inhibited osteogenic differentiation in MC3T3-E1 cells [58]. However, our results showed that *Bmp2* mRNA and protein expression were increased by LiCl in BMSCs. This discrepancy may be ascribed to the difference in cell types and stimulation received, which should be included in further studies.

Previous studies have indicated that autophagy inhibits apoptosis, thus favoring the survival status of cells [59]. Inhibited autophagy can coordinate with endoplasmic reticulum stress, resulting in apoptosis [60]. LiCl has been reported to inhibit apoptosis through the regulation of GSK-3 β [61]. In this study, we found that increased autophagy induced by LiCl reversed ovariectomy-induced apoptosis both in vivo and in vitro, indicating that autophagy may play a positive role in BMSCs and OTM processes to prevent apoptosis [62]. In bone tissue metabolism, autophagy is involved in regulating the survival and functioning of osteocytes, osteoblasts, and osteoclasts [54]. Moreover, studies have also showed that the bone turnover related to the other ions

such as strontium and calcium, yet there is a lack of evidence regarding these ions and autophagy [63,64]. Further studies are needed to elucidate the potential role of autophagy via ions in regulating these cells during OTM. It has been reported that autophagy also has a meaningful influence on bone homeostasis by regulating the RANKL/OPG axis [65]. Our results showed increased Beclin-1 and LC3II expression and decreased p62 protein levels in BMSCs following LiCl administration, accompanied by a significant upregulation of the OPG/RANKL ratio ($P = 0.001$, Supplementary Table 5). These findings are consistent with the findings observed in LiCl-treated mice, further indicating that LiCl may protect against osteoclastogenesis caused by osteoporosis during OTM via the RANKL/OPG pathway.

In the current study, we examined the effect of LiCl on autophagy and its correlation with apoptosis and bone remodeling under osteoporotic conditions in mice and BMSCs (Fig. 8). LiCl resulted in upregulation of autophagy activity. The expression of osteogenesis-related biomarkers was upregulated and apoptosis was downregulated, demonstrating that autophagy activation favored osteogenesis and bone formation with LiCl administration. However, this study is only an explorative study on the promotion effect of LiCl on autophagy and its role in the regulation of apoptosis and bone remodeling during OTM in osteoporotic mice. As such, further research is required to determine the specific mechanism of autophagy activation on bone remodeling. One limitation of our study is that LiCl was systemically applied in mice, which might have side effects on other tissues and organs [66]. Ongoing studies based on the local application of LiCl during OTM should be considered to resolve this limitation.

5. Conclusion

This study is the first to demonstrate that LiCl can promote bone formation in ovariectomized mice during OTM. Our results indicated that LiCl activated osteogenesis and inhibited apoptosis in osteoporotic BMSCs by positively regulating autophagy. These findings broaden our understanding of the biological mechanisms that occur during OTM in individuals with osteoporosis. Our study provides evidence to support the use of LiCl in providing safe orthodontic treatment to osteoporotic patients with better and more controllable outcomes.

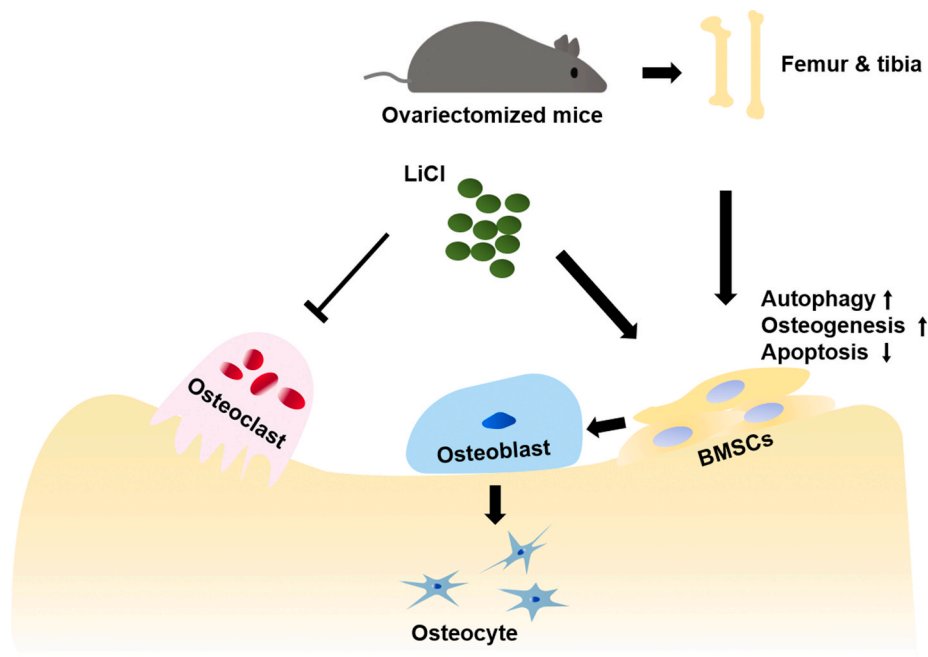


Fig. 8. Working model for LiCl function in the regulation of osteogenesis. LiCl rejuvenated the osteogenic differentiation of OVX BMSCs by upregulation of autophagy, downregulation of apoptosis and inhibition of osteoclastic activity in the alveolar bone.

Funding

This work was supported by National Natural Science Foundation of China (Grants No. 81801019, 81701032, 82071150), and National Key Research and Development Program of China (Grant No. 2018YFC1105703).

CRediT authorship contribution statement

Li Huang: Conceptualization, Investigation, Methodology, Project administration, Writing – original draft. **Xing Yin:** Data curation, Funding acquisition, Investigation, Writing – review & editing. **Jun Chen:** Methodology, Investigation, Software. **Ruojing Liu:** Data curation, Methodology, Resources. **Xiaoyue Xiao:** Data curation, Methodology, Software. **Zhai Hu:** Resources, Methodology, Writing – review & editing. **Yan He:** Data curation, Formal analysis, Investigation, Writing – review & editing. **Shujuan Zou:** Project administration, Funding acquisition, Supervision, Writing – review & editing.

Declaration of competing interest

The authors declare that there are no known conflicts of interest in this study.

Appendix A. Supplementary data

Supplementary data to this article can be found online at <https://doi.org/10.1016/j.bioactmat.2021.02.015>.

References

- [1] Osteoporosis on mayo clinic web. <https://www.mayoclinic.org/diseases-conditions/osteoporosis/symptoms-causes/syc-20351968>, 2019.
- [2] W. Liu, et al., GDF11 decreases bone mass by stimulating osteoclastogenesis and inhibiting osteoblast differentiation, *Nat. Commun.* 7 (2016) 12794.
- [3] Q. Dai, et al., Force-induced increased osteogenesis enables accelerated orthodontic tooth movement in ovariectomized rats, *Sci. Rep.* 7 (1) (2017) 3906.
- [4] S. Sidiropoulou-Chatzigiannis, M. Kourtidou, L. Tsalikis, The effect of osteoporosis on periodontal status, alveolar bone and orthodontic tooth movement. A literature review, *J. Int. Acad. Periodontol.* 9 (3) (2007) 77–84.
- [5] J. Huang, et al., Myricetin prevents alveolar bone loss in an experimental ovariectomized mouse model of periodontitis, *Int. J. Mol. Sci.* 17 (3) (2016) 422.
- [6] X. Yin, et al., Autophagy in bone homeostasis and the onset of osteoporosis, *Bone Research* 7 (1) (2019).
- [7] K. Mochida, et al., Receptor-mediated selective autophagy degrades the endoplasmic reticulum and the nucleus, *Nature* 522 (7556) (2015) 359–362.
- [8] H. Wei, J.L. Guan, Blocking tumor growth by targeting autophagy and SQSTM1 in vivo, *Autophagy* 11 (5) (2015) 854–855.
- [9] R.L. Jilka, C.A. O'Brien, The role of osteocytes in age-related bone loss, *Curr. Osteoporos. Rep.* 14 (1) (2016) 16–25.
- [10] G. Kroemer, Autophagy: a druggable process that is deregulated in aging and human disease, *J. Clin. Invest.* 125 (1) (2015) 1–4.
- [11] M. Onal, et al., Suppression of autophagy in osteocytes mimics skeletal aging, *J. Biol. Chem.* 288 (24) (2013) 17432–17440.
- [12] D.C. Rubinsztein, G. Marino, G. Kroemer, Autophagy and aging, *Cell* 146 (5) (2011) 682–695.
- [13] M. Bonyadi, et al., Mesenchymal progenitor self-renewal deficiency leads to age-dependent osteoporosis in Sca-1/Ly-6A null mice, *Proc. Natl. Acad. Sci. Unit. States Am.* 100 (10) (2003) 5840–5845.
- [14] T.R. O'Donovan, et al., Lithium modulates autophagy in esophageal and colorectal cancer cells and enhances the efficacy of therapeutic agents in vitro and in vivo, *PLoS One* 10 (8) (2015) e0134676.
- [15] L. Wang, et al., Glucocorticoids induce autophagy in rat bone marrow mesenchymal stem cells, *Mol. Med. Rep.* 11 (4) (2015) 2711–2716.
- [16] R. Xu, et al., Simvastatin improves oral implant osseointegration via enhanced autophagy and osteogenesis of BMSCs and inhibited osteoclast activity, *J Tissue Eng Regen Med* 12 (5) (2018) 1209–1219.
- [17] W. Young, Review of lithium effects on brain and blood, *Cell Transplant.* 18 (9) (2009) 951–975.
- [18] A. Del Grosso, et al., Lithium improves cell viability in psychosine-treated MO3.13 human oligodendrocyte cell line via autophagy activation, *J. Neurosci. Res.* 94 (11) (2016) 1246–1260.
- [19] S. Sarkar, et al., Lithium induces autophagy by inhibiting inositol monophosphatase, *J. Cell Biol.* 170 (7) (2005) 1101–1111.
- [20] P. Clement-Lacroix, et al., Lrp5-independent activation of Wnt signaling by lithium chloride increases bone formation and bone mass in mice, *Proc. Natl. Acad. Sci. U. S. A.* 102 (48) (2005) 17406–17411.
- [21] Z. Zhu, et al., Lithium stimulates human bone marrow derived mesenchymal stem cell proliferation through GSK-3beta-dependent beta-catenin/Wnt pathway activation, *FEBS J.* 281 (23) (2014) 5371–5389.
- [22] J. Pan, et al., Lithium enhances alveolar bone formation during orthodontic retention in rats, *Orthod. Craniofac. Res.* 20 (3) (2017) 146–151.
- [23] H. Kazemi, et al., Lithium prevents cell apoptosis through autophagy induction, *Bratisl. Lek. Listy* 119 (4) (2018) 234–239.
- [24] L. Song, et al., Optimization of the time window of interest in ovariectomized imprinting control region mice for antiosteoporosis research, *BioMed Res. Int.* 2017 (2017), 8417814.
- [25] F. Li, et al., Effect of parathyroid hormone on experimental tooth movement in rats, *Am. J. Orthod. Dentofacial Orthop.* 144 (4) (2013) 523–532.

- [26] G.H. Tang, et al., Lithium delivery enhances bone growth during midpalatal expansion, *J. Dent. Res.* 90 (3) (2011) 336–340.
- [27] X. Wang, et al., Systemic administration of lithium improves distracted bone regeneration in rats, *Calcif. Tissue Int.* 96 (6) (2015) 534–540.
- [28] J. Zhang, et al., Repair of critical-sized mandible defects in aged rat using hypoxia preconditioned BMSCs with up-regulation of hif-1 alpha, *Int. J. Biol. Sci.* 14 (4) (2018) 449–460.
- [29] H.J. Jiang, et al., Tenuigenin promotes the osteogenic differentiation of bone mesenchymal stem cells in vitro and in vivo, *Cell Tissue Res.* 367 (2) (2017) 257–267.
- [30] Z.P. Ma, et al., Effects of the 1, 4-dihydropyridine L-type calcium channel blocker benidipine on bone marrow stromal cells, *Cell Tissue Res.* 361 (2) (2015) 467–476.
- [31] P. Gao, et al., Salvianolic acid B improves bone marrow-derived mesenchymal stem cell differentiation into alveolar epithelial cells type I via Wnt signaling, *Mol. Med. Rep.* 12 (2) (2015) 1971–1976.
- [32] Z. Yu, et al., Lithium chloride attenuates the abnormal osteogenic/adipogenic differentiation of bone marrow-derived mesenchymal stem cells obtained from rats with steroid-related osteonecrosis by activating the beta-catenin pathway, *Int. J. Mol. Med.* 36 (5) (2015) 1264–1272.
- [33] A. Coker-Gurkan, et al., Inhibition of autophagy by 3-MA potentiates purvalanol-induced apoptosis in Bax deficient HCT 116 colon cancer cells, *Exp. Cell Res.* 328 (1) (2014) 87–98.
- [34] L. Chen, S. Mo, Y. Hua, Compressive force-induced autophagy in periodontal ligament cells downregulates osteoclastogenesis during tooth movement, *J. Periodontol.* 90 (10) (2019) 1170–1181.
- [35] R. Kang, et al., The Beclin 1 network regulates autophagy and apoptosis, *Cell Death Differ.* 18 (4) (2011) 571–580.
- [36] L.C. Hofbauer, C.A. Kuhne, V. Viereck, The OPG/RANKL/RANK system in metabolic bone diseases, *J. Musculoskelet. Neuronal Interact.* 4 (3) (2004) 268–275.
- [37] G. Han, et al., Effects of simvastatin on relapse and remodeling of periodontal tissues after tooth movement in rats, *Am. J. Orthod. Dentofacial Orthop.* 138 (5) (2010) 550 e1–7, discussion 550–1.
- [38] J.A. Kanis, et al., The diagnosis of osteoporosis, *J. Bone Miner. Res.* 9 (8) (1994) 1137–1141.
- [39] M. Salazar, et al., Effect of alendronate sodium on tooth movement in ovariectomized rats, *Arch. Oral Biol.* 60 (5) (2015) 776–781.
- [40] S.G. Arslan, et al., Effects of estrogen deficiency on tooth movement after force application: an experimental study in ovariectomized rats, *Acta Odontol. Scand.* 65 (6) (2007) 319–323.
- [41] Q.G. Dai, et al., Ovariectomy induces osteoporosis in the maxillary alveolar bone: an in vivo micro-CT and histomorphometric analysis in rats, *Oral Dis.* 20 (5) (2014) 514–520.
- [42] B. Chen, et al., Zoledronic acid enhances bone-implant osseointegration more than alendronate and strontium ranelate in ovariectomized rats, *Osteoporos. Int.* 24 (7) (2013) 2115–2121.
- [43] B.N. Souza-Silva, et al., The influence of teriparatide in induced tooth movement: a systematic review, *J Clin Exp Dent* 8 (5) (2016) e615–e621.
- [44] S. Krishnan, S. Pandian, S.A. Kumar, Effect of bisphosphonates on orthodontic tooth movement—an update, *J. Clin. Diagn. Res.* 9 (4) (2015) ZE01–5.
- [45] M. Arioka, et al., Acceleration of bone regeneration by local application of lithium: Wnt signal-mediated osteoblastogenesis and Wnt signal-independent suppression of osteoclastogenesis, *Biochem. Pharmacol.* 90 (4) (2014) 397–405.
- [46] D. Geng, et al., Pharmaceutical inhibition of glycogen synthetase kinase 3 beta suppresses wear debris-induced osteolysis, *Biomaterials* 69 (2015) 12–21.
- [47] Y. Chen, et al., Beta-catenin signaling plays a disparate role in different phases of fracture repair: implications for therapy to improve bone healing, *PLoS Med.* 4 (7) (2007) e249.
- [48] Y. Jin, et al., Lithium chloride enhances bone regeneration and implant osseointegration in osteoporotic conditions, *J. Bone Miner. Metabol.* 35 (5) (2017) 497–503.
- [49] A. Ino-Kondo, et al., Lithium chloride reduces orthodontically induced root resorption and affects tooth root movement in rats, *Angle Orthod.* 88 (4) (2018) 474–482.
- [50] C. Wang, et al., HOXA10 inhibit the osteogenic differentiation of periodontal ligament stem cells by regulating beta-catenin localization and DKK1 expression, *Connect Tissue Res.* 2020, pp. 1–9.
- [51] E. Nemoto, et al., Wnt signaling inhibits cementoblast differentiation and promotes proliferation, *Bone* 44 (5) (2009) 805–812.
- [52] Y. Motoi, et al., Lithium and autophagy, *ACS Chem. Neurosci.* 5 (6) (2014) 434–442.
- [53] D. Nie, et al., Lithium chloride (LiCl) induced autophagy and downregulated expression of transforming growth factor beta-induced protein (TGFB1) in granular corneal dystrophy, *Exp. Eye Res.* 173 (2018) 44–50.
- [54] M. Nollet, et al., Autophagy in osteoblasts is involved in mineralization and bone homeostasis, *Autophagy* 10 (11) (2014) 1965–1977.
- [55] K. Matsunaga, et al., Two Beclin 1-binding proteins, Atg14L and Rubicon, reciprocally regulate autophagy at different stages, *Nat. Cell Biol.* 11 (4) (2009) 385–396.
- [56] Y. Kabeya, et al., LC3, a mammalian homologue of yeast Apg8p, is localized in autophagosome membranes after processing, *EMBO J.* 19 (21) (2000) 5720–5728.
- [57] M. Qi, et al., Autophagy maintains the function of bone marrow mesenchymal stem cells to prevent estrogen deficiency-induced osteoporosis, *Theranostics* 7 (18) (2017) 4498–4516.
- [58] J. Li, et al., Lithium chloride attenuates BMP-2 signaling and inhibits osteogenic differentiation through a novel WNT/GSK3- independent mechanism, *Bone* 48 (2) (2011) 321–331.
- [59] N. Cai, et al., Autophagy protects against palmitate-induced apoptosis in hepatocytes, *Cell Biosci.* 4 (2014) 28.
- [60] I. Szumiel, Autophagy, reactive oxygen species and the fate of mammalian cells, *Free Radic. Res.* 45 (3) (2011) 253–265.
- [61] J.E. Forde, T.C. Dale, Glycogen synthase kinase 3: a key regulator of cellular fate, *Cell. Mol. Life Sci.* 64 (15) (2007) 1930–1944.
- [62] Y. Liu, et al., Autophagy protects bone marrow mesenchymal stem cells from palmitate-induced apoptosis through the ROS/JNK/p38 MAPK signaling pathways, *Mol. Med. Rep.* 18 (2) (2018) 1485–1494.
- [63] H. Xie, et al., Microenvironment construction of strontium–calcium-based biomaterials for bone tissue regeneration: the equilibrium effect of calcium to strontium, *J. Mater. Chem. B* 6 (15) (2018) 2332–2339.
- [64] Xie, H., et al., A novel bioceramic scaffold integrating silk fibroin in calcium polyphosphate for bone tissue-engineering. *Ceram. Int.* 42(2): p. 2386-2392.
- [65] H. Li, et al., Defective autophagy in osteoblasts induces endoplasmic reticulum stress and causes remarkable bone loss, *Autophagy* 14 (10) (2018) 1726–1741.
- [66] S.W. Lehmann, J. Lee, Lithium-associated hypercalcemia and hyperparathyroidism in the elderly: what do we know? *J. Affect. Disord.* 146 (2) (2013) 151–157.